This article has been accepted for publication in a future issue of this journal, but has not been fully edited. Content may change prior to final publication. Citation information: DOI 10.1109/TWC.2018.2817481, IEEE Transactions on Wireless Communications

Cooperative Device-to-Device Communication for Uplink Transmission in Cellular System

Yue Li and Lin Cai, *Senior Member, IEEE*

***Abstract*—The rapid development of the Internet of things has brought new challenges to cellular networks with super-dense devices and deep-fading channels. These challenges may substantially decrease the transmission efficiency and increase the device's power consumption, especially in the uplink. A pressing issue is to improve enhanced Node B's (eNB) scheduler considering a large number of users. In this paper, a semi-centralized cooperative control method is proposed for the cellular uplink transmissions, where the User Equipment (UE) relays are randomly selected according to a certain density decided by the eNB. Two specific cooperative schemes based on Device-to-Device (D2D) communications are proposed, which are the random UE relay scheme and the one further applying network coding. The D2D interference is considered and modelled based on stochastic geometry. The proposed schemes are analyzed based on two distinct traffic models, i.e., the MTC traffic with the small-data feature and the full-buffer traffic. Extensive Monte Carlo simulations have been conducted for the small-data traffic and the closed-form theoretical results have been derived for the full-buffer traffic. Performance gains are achieved in various scenarios and the comparisons between two cooperative schemes are made as well. The results provide an important guideline for the eNB to determine how to select and configure cooperative D2D communication for uplink.**

I. Introduction

The rapid development of the Internet of Things (IoT) has brought new challenges to cellular networks due to super-dense Machine Type Communications (MTC) devices [3] and deep fading channels [4]. Serving a large number of the MTC devices will impose a huge pressure on the scheduler of the enhanced Node B (eNB). In addition, due to the complicated deployments and channel impairments for indoor/underground devices, one single transmission may need hundreds of repetitions to meet the link budget [4], which is especially undesirable for the MTC devices with limited energy supply [3]. Also, inefficient repetitions will occupy a large portion of the cellular resources and lead to performance degradation of the whole network.

MTC traffic typically has a certain degree of delay tolerance [5]. Overshooting the Quality of Service (QoS) requirements may result in resource waste. Therefore, the main objective of this paper is to increase the transmission efficiency in cellular uplink while reducing the pressure on eNB's scheduler and devices' power consumption by exploring the delay tolerance feature of the MTC traffic. In this paper, a semi-centralized cooperative control method is proposed to reduce the control/feedback overhead, where the User Equipment (UE) relays are randomly selected according to the density decided by the eNB. We adopt both the random UE relay scheme and the one further applying Network Coding (NC) for cooperation, where the feature of delay tolerance is exploited by local packet exchange and the transmission efficiency is improved thanks to the multi-user diversity gain.

Two distinct traffic models, i.e., the MTC traffic with the small-data feature [3] and the full-buffer traffic, are applied to examine the proposed schemes. In the current LTE/LTE-A system, the minimum resource allocation unit is one Physical Resource Block (PRB). If the packet size from the MTC device is too small, it cannot fully utilize one PRB especially when the channel condition is good to apply a higher-order Modulation and Coding Scheme (MCS). This motivates us to investigate the effects of the proposed schemes for the MTC small-data traffic. Meanwhile, it is also worthy to examine the proposed schemes for other traffic models without the small-data feature when the small-data aggregation gain does not exist. Thus, the full-buffer traffic is considered. In the MTC scenarios, continuous data coming from delay insensitive videos and high resolution pictures can be modeled as full-buffer traffic.

The main contributions of this paper are four-fold. First, we have proposed an efficient semi-centralized cooperative control method for the uplink transmissions in cellular systems. Two specific cooperative schemes based on D2D have been proposed: one is the random UE relay scheme and the other further applies NC. The proposed schemes can substantially increase the transmission efficiency while reducing the overhead, scheduling queue length, and devices' power consumption. Second, a feasible system design including the protocol stack has been given, which is backward-compatible with the current LTE/LTE-A system and easy to implement. Third, the system has been modeled based on two distinct traffic models, i.e., the MTC small-data traffic and the full-buffer traffic. The D2D interference is considered and modeled applying stochastic geometry. Fourth, extensive simulations have been conducted for the MTC small-data traffic in various scenarios to identify the performance gain and compared the two cooperative schemes. The performance with full-buffer traffic has been analyzed theoretically, and the closed-form results have been obtained. Extensive numerical evaluations are then performed. These results provide important guidelines for the eNB, such as when each of cooperative scheme is preferable, and how to

Yue Li and Lin Cai are with the Department of Electrical and Computer Engineering, University of Victoria, BC V8P 5C2, Canada (e-mail: liyue331@uvic.ca; cai@uvic.ca).

Manuscript received May 4, 2017; revised October 27, 2017, January 23, 2018; accepted March 15, 2018.

Part of this work has been presented at the Vehicular Technology Conference (VTC-Fall 2016) [1] and the Global Communications Conference (GLOBECOM 2016) [2].

This article has been accepted for publication in a future issue of this journal, but has not been fully edited. Content may change prior to final publication. Citation information: DOI 10.1109/TWC.2018.2817481, IEEE Transactions on Wireless Communications

approximately determine the optimal density of the UE relays.

The rest of the paper is organized as follows. The related work is summarized in Sec. II. In Sec. III, the system designs are described. Sec. IV presents the system model, including the channel model, the scheduling algorithm and the D2D interference model for the MTC small-data traffic. Corresponding simulation results are given in Sec. V. The theoretical analysis and numerical evaluations for the full-buffer traffic are shown in Sec. VI and Sec. VII, respectively, followed by the concluding remarks and possible future work in Sec. VIII.

II. Related Work

The D2D communication was first introduced by the 3rd Generation Partnership Project (3GPP) as Proximity-based Services (ProSe) [6], which was originally proposed to disseminate critical messages in disasters. The same transmission mechanism also is applicable for other use cases such as local data exchange, UE relay, and converged heterogeneous network [7], [8].

Cooperative transmission based on UE relay and D2D is a promising technique to improve the transmission efficiency and extend the cellular transmission range [9], [10]. It is suitable for delay-tolerant traffic because additional delay is introduced by local data exchanges. A detailed protocol for the downlink cooperative transmission was designed in [11], where the multi-user diversity gain can be obtained. In [12], the uplink case was studied, where the eNB selects the best UE relay but the global information is needed which increases the feedback load when the number of users is large. D2D interference cannot be ignored due to the fact that D2D transmissions will reuse the cellular uplink resource. It was analyzed based on stochastic geometry in [13], [14]. A relay node selection method based on the D2D interference was proposed in [15], which also requires global information.

Another efficient way for cooperative transmission is to use NC, which has been extensively studied recently [16]–[19]. The senders combine several original packets and generate new packets using the linear combinations of them. The coefficients and operations are in a Galois field. Once the number of linear combinations received constitute a full-rank matrix, the receiver can recover the original packets by solving a system of linear equations.

NC and D2D were combined for local data exchange [20] and cellular transmissions [21]. The Random Linear Network Coding (RLNC) was applied for the cellular multicast channel in [22], [23], and the multiple unicast scenario was studied in [24]. Most of the research on combining NC and D2D focused on downlink broadcast/multicast scenarios [25], and a detailed protocol design based on LTE system was proposed in [26]. In [27], the basic NC scheme and a grouping method based on two users' complementary channels were introduced for uplink transmissions. [28] focused on a single link and applied NC for the UE relay node to combine the packets from the eNB, the edge UE, and the relay UE, which is different from our scenario.

Different from the previous work, in this paper, we target on the cellular uplink transmissions, and apply the semi-centralized grouping method based on the largest receiving power in the D2D links, which reduces the overhead as well as guarantees the quality of the D2D transmissions. Besides, both theoretical and numerical analyses are given from the system perspective, where the scheduling and interference are considered, rather than focusing on a single link.

III. System Design

A. Transmission Procedure Design

The eNB broadcasts a parameter a ($\in [0,1]$) to all of the MTC UEs. Each UE can become a D2D agent according to a certain probability which is a function of a. A simple implementation is that each UE draws a random number between 0 and 1 and checks whether the random number is smaller than a to be a D2D agent, which is similar to the legacy Access Class Barring (ACB) scheme in LTE/LTE-A. The UEs other than the D2D agents are named as capillary UEs.

We adopt the ACB-like scheme because of the control overhead concern. If the eNB designates specific UEs as the D2D agents, first the eNB needs to collect all the requests from all active UEs and then the control information has to be sent back. It takes a long time and occupies a large amount of resources. This tedious procedure has to be repeated whenever the topology or the traffic changes and the groups need to be reformed. It is inefficient for the eNB to control the network with massive number of MTC UEs. On the contrary, there is only one parameter a being sent on the broadcast channel in the proposed scheme.

Once the D2D agents are selected, each D2D agent broadcasts a preamble via D2D with a fixed transmitting power. All the capillary UEs find the nearest D2D agents according to the receiving power of the D2D preambles, and then establish the D2D connections.

The D2D preambles are sent in the predetermined cellular uplink resources. All the D2D agents are synchronized by the eNB's downlink broadcasting channel, and the D2D preamble transmission procedure is triggered by either the updating of a or other broadcast notifications. Given that the eNB controls the timing of the preamble transmissions, it shall schedule the uplink cellular transmissions to allocate resources for preamble transmissions. During the time period that the topology is relatively stable, no D2D preamble or grouping is needed, until a number of new UEs arriving to the system and cannot find suitable D2D agent nearby. For the MTC scenario, given the fixed location of the devices, the overhead of preamble transmission and grouping is tolerable.

The D2D preamble transmissions may be spread using orthogonal code, time, and frequency to reduce the collision probability. The regular preamble structure in LTE system can be adopted, which includes 64 orthogonal Zadoff-Chu sequences. Similar to the Physical Random Access Channel (PRACH) structure in LTE, we can predetermine multiple frequency bands and sub-frames for the D2D preamble transmissions. Each D2D agent shall randomly select a Zadoff-Chu sequence, a frequency band, and a sub-frame. Given the limited transmission range of the preamble and the orthogonal

This article has been accepted for publication in a future issue of this journal, but has not been fully edited. Content may change prior to final publication. Citation information: DOI 10.1109/TWC.2018.2817481, IEEE Transactions on Wireless Communications

resources used, the D2D preamble collisions can be well controlled.

If the location information is available, a capillary UE can select the nearest D2D agent by calculating the distance. Otherwise, according to the receiving power of the preambles, a capillary UE shall find the D2D agent corresponding to the highest average receiving power, which typically corresponds to the shortest transmission distance because the path loss may dominate the channel gain. Therefore, in the analysis, we assume that all the capillary UEs can find the nearest D2D agent for simplification.

Once a UE decides to connect the D2D agent, it shall exchange signaling messages with the D2D agent on specified resources. The resources can be implied by the selected Zadoff-Chu sequence and resource for the D2D preamble transmission. During the signaling exchange, the D2D preamble collisions can be further resolved, as well as the collisions among the capillary UEs in the same group. Besides, other parameters related to D2D data transmission can be negotiated, such as the maximum transmitting power and a predetermined schedule pattern inside the group. There are two types of collisions. One is the collision among different D2D agents, i.e., they select the same preamble and resource. Another one is the collision among capillary UEs in the same group, i.e, they are using the same resource to send signaling to the D2D agent. For the first one, random sequences generated by D2D agents (or their unique ID) are piggybacked in signaling and sent back to capillary UEs. If collision happens and a UE fails to decode the signaling, it shall notify that to the D2D agents. Thus, the colliding D2D agents can be aware of collisions and redo the preambles and resource selection. For the collision among capillary UEs, the random sequence can also be piggybacked, which is the same as the current contention-based random access mechanism in LTE system.

Each D2D agent and its connected capillary UEs can be considered as a cooperation group. We assume that the UEs' locations in a macro cell follow a Poisson Point Process (PPP), given the thinning procedure, the locations of the randomly selected D2D agents also follow a PPP. The macro area can be divided into many Voronoi cells, and each Voronoi cell contains one cooperation group. According to different traffic situations and UE densities, the probability of a UE becoming a D2D agent can be updated by the eNB.

In one Voronoi cell, there are two cooperative schemes for the uplink transmission. The first one is the NC scheme, as shown in Fig. 1 (a), where the D2D agent collects original packets from each capillary UE and then broadcasts all the packets back to the capillary UEs through the D2D network, so that each UE obtains all the packets of other UEs in this Voronoi cell. No matter which UE is scheduled, it will always transmit linear combinations of all the original packets. Therefore, the eNB can select the UE with the best channel condition in a Voronoi cell to transmit in the uplink, by which the multi-user diversity gain can be achieved.

The second scheme is shown in Fig. 1 (b) and is considered as the Random UE Relay (RUR) scheme in this paper. The main difference is that the D2D agent will not broadcast the packets back to the capillary UEs and only the D2D agent

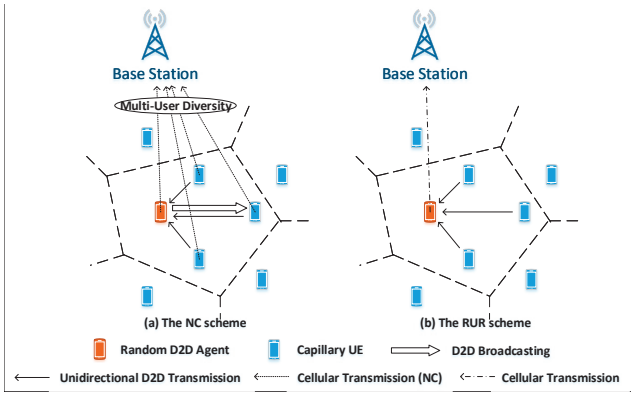

Fig. 1. Two alternative semi-centralized control methods.

can be scheduled for the cellular uplink transmission (original packets are transmitted). The RUR scheme can obtain the benefit of small-packet aggregation, but it cannot achieve the multi-user diversity gain. On the other hand, the signaling and feedback overhead is significantly reduced, because the eNB does not need to know the channel conditions and other status of the capillary UEs. Also, due to a fewer number of D2D transmissions, the D2D interference level is reduced. Without a careful study, it is difficult to conclude which solution can achieve a better performance in a specific scenario.

It is possible to further explore the multi-user diversity gain in the RUR scheme by applying the dynamic scheduling within a group. However, coordinating all capillary UEs to send the packets to the scheduled UE dynamically can be costly and time-consuming, and thus becomes infeasible. Note that in FDD-LTE, the time for the scheduled UE to prepare the uplink transmission after receiving the scheduling message is 4ms only. Alternatively, each UE can store other's packets beforehand, which generates the same D2D traffic load and interference as the NC scheme. From the received SINR's point of view, this method has the same performance as the NC scheme (the same diversity gain and the same D2D interference), but the NC scheme can reduce the control overhead thanks to its insensitiveness to the order of the (re)transmissions. The analytical results on the NC scheme can be considered as the upper-bound of applying dynamic scheduling.

We propose the NC scheme because it can effectively explore the multi-user diversity and small data aggregation gains, which improves the transmission efficiency, without introducing additional control overhead in regard of the re-transmission and reordering. We propose the RUR scheme because it minimizes the control/feedback overhead and reduce the complexity of the eNB while maintaining the small data aggregation gain. The proposed schemes do not use multi-antenna techniques which may not be applicable for MTC devices. The transmission efficiency and the overhead/complexity due to massive MTC devices are two major issues to be addressed in the cellular system. We propose these two cooperative schemes to deal with them, respectively. Our analysis provides good guidelines to make the trade-off to select the

This article has been accepted for publication in a future issue of this journal, but has not been fully edited. Content may change prior to final publication. Citation information: DOI 10.1109/TWC.2018.2817481, IEEE Transactions on Wireless Communications

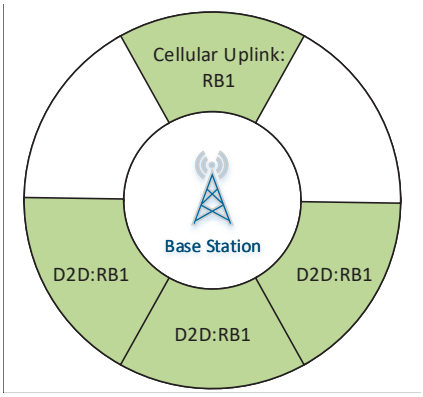

Fig. 2. An example of the D2D resource allocation.

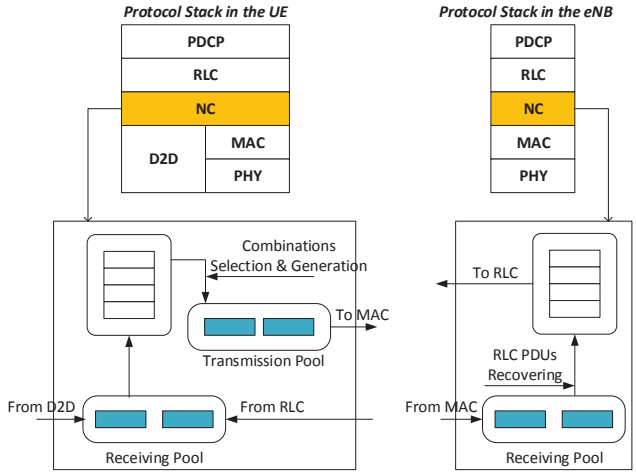

Fig. 3. Design of the cellular air interface protocol stack.

better scheme in different scenarios.

B. D2D Resource Allocation

In this paper, we assume that the D2D transmissions are exactly underlying with cellular uplink transmissions, so no additional resource is occupied by D2D and thus a fair comparison with the legacy system can be made. There is a mutual interference between D2D and cellular uplink transmissions and the resource allocation for the D2D has a great impact on the performance.

We assume that the eNB can mitigate the interference by a careful scheduling. A simple example of the scheduling is shown in Fig. 2, where we consider one PRB as the scheduling unit. The whole macro cell area can be divided into several sectors. When one PRB is occupied by a UE for cellular uplink transmissions, the sectors far away from it can reuse this PRB for D2D transmissions. Therefore, because of the relatively long distance, the interference from a cellular transmission to the D2D users is negligible in this work. However, the distances to the eNB are similar for both the cellular UEs and the D2D UEs, so that the interference from D2D transmissions to cellular uplink transmissions cannot be neglected, which is modeled according to the worst case in the following sections.

C. Protocol Design

In the RUR scheme, the D2D agent acts as a UE relay. Most of the functions used in this scheme are either supported by the current LTE/LTE-A system or coming cellular standards such as the ProSe project in 3GPP [29]. For the capillary UE, it shall simply send the packets to the D2D agent. The D2D agent stores the packets from different capillary UEs in different dedicated Radio Link Control (RLC) entities. Once scheduled, it generates the Media Access Control (MAC) Protocol Data Unit (PDU) by multiplexing PDUs from different RLC entities according to the existing LTE priority handling algorithm [30].

For the NC scheme, we insert a NC layer as shown in Fig. 3. Similarly to the first step of the RUR scheme, all the capillary UEs send their packets (RLC PDUs) to the D2D agent. Then, the D2D agent broadcasts all the received packets, as well as its own packets, back to the capillary UEs. By now, all the packets need to be transmitted are stored by every UE in the group. When scheduled, the UE uses the packets stored in the receiving pool to generate the linear combinations and sends them to the eNB. We propose to define several coefficient tables according to various dimensions in specifications. In each table, linear independence is the guideline to design the detailed values of coefficient vectors. As long as N (the number of original packets) different coefficient vectors are linearly independent to each other, they can always build an invertible (full-rank) matrix, and thus Gauss-Jordan elimination can be applied to recover the original packets. A unique index is assigned to each coefficient vector in the table. There are many options in the current system to inform UEs the index without introducing additional overhead, such as implicitly inferring from the System Frame Number (SFN), i.e., each SFN can be converted to a unique index, or using the index in a deterministic order. In order to facilitate the linear operation among packets, the fix-size RLC PDU is applied.

In the LTE/LTE-A system, the ciphering/deciphering is performed in the Packet Data Convergence Protocol (PDCP) layer. In the NC scheme, though UEs received RLC PDUs from others, they cannot decipher the PDCP Service Data Units (SDUs) in the PDCP layer because they do not have others' keys. The keys used in the PDCP layer are negotiated by Non-Access Stratum (NAS) messages which are independent to the proposed schemes. Thus, our design can ensure that the existing security function in Radio Access Network (RAN) is preserved.

IV. System Model For The MTC Small-Data Traffic

In this section, we consider the two-layer scheduling including the macro cell scheduling and that within one single Voronoi cell, and give the channel models for both cellular and D2D transmissions. After that, the D2D interference is modeled based on the stochastic geometry and the characteristics of the MTC small-data traffic.

This article has been accepted for publication in a future issue of this journal, but has not been fully edited. Content may change prior to final publication. Citation information: DOI 10.1109/TWC.2018.2817481, IEEE Transactions on Wireless Communications

A. Scheduling

In the macro cell scheduling, the users' fairness should be considered. The proportional fairness (PF) scheduling algorithm has been widely adopted, which can provide a reasonable trade-off between the throughput and fairness [31]. Considering the heterogeneous channel case, i.e., i.ni.d channels for different users, an alternative normalized signal-to-noise ratio (SNR) scheduling algorithm can be used [32], [33], i.e.,

$$k^{(*)} = \arg\max_{k} \left\{ \frac{\gamma_k}{\bar{\gamma}_k} \right\}, \tag{1}$$

where γ_k and $\bar{\gamma}_k$ are the kth UE's instantaneous and average SNR, respectively. $k^{(*)}$ denotes the scheduled UE.

We use the normalized SNR scheduling in the macro cell. Therefore, it can be assumed that there are several equivalent UEs in a macro cell, whose number equals the number of Voronoi cells in the macro cell. There is another layer of scheduling for the NC scheme. The Max C/I scheduling algorithm is adopted in a Voronoi cell, as shown below, so that the scheduled SNR of each equivalent UE will be the same as the best UE in that Voronoi cell.

$$k^{(*)} = \arg\max_{k} \{\gamma_k\}. \tag{2}$$

For the RUR scheme, there is no scheduling in a Voronoi cell. The SNR of each equivalent UE is the SNR of the D2D agent in that Voronoi cell.

B. Channel Models

We assume independent log-normal shadowing and Rayleigh fading for each UE. Given that there are M capillary UEs in the ith Voronoi cell. The Cumulative Distribution Function (CDF) of the received SNR $\gamma^{(j,i)}$ in the eNB side from the jth UE, $j = 1, 2, ..., M+1$, in the ith Voronoi cell can be given by

$$F_{\gamma^{(j,i)}}(r \mid \bar{\gamma}_j) = 1 - e^{\frac{-r}{\bar{\gamma}_j}}, \tag{3}$$

where $\bar{\gamma}_j$ is the average SNR and is also a random variable follows log-normal distribution $\ln \mathcal{N}(\mu_i, \sigma)$ due to shadowing effect, which means $\bar{\gamma}_j$ is the average of small-scale fading. $F_{\gamma^{(j,i)}}(r \mid \bar{\gamma}_j)$ is the CDF of $\gamma^{(j,i)}$ given a fixed average SNR $\bar{\gamma}_j$. Its standard notation is $P(\gamma^{(j,i)} \leq r \mid \bar{\gamma}_j = x) = 1 - e^{\frac{-r}{x}}$, in order to simplify the notations in the following sections, we adopt the form shown in (3). We assume that UEs in the same Voronoi cell have approximately the same distance to the eNB. Therefore, $\mu_i = \bar{\gamma}(d_i)$, where $\bar{\gamma}(d_i)$ denotes the average received SNR based on the path loss and is a function of the distance from the ith Voronoi cell to the eNB, d_i. Given a fixed d_i, the CDF of $\bar{\gamma}_j$ is given by

$$F_{\bar{\gamma}_j}(x \mid d_i) = \Phi\left(\frac{10 \log_{10} x/\bar{\gamma}(d_i)}{\sigma} \right), \tag{4}$$

where $\Phi(\cdot)$ is the CDF of the standard normal distribution.

In this section, as we consider the MTC small-data traffic generated by indoor/undergroud devices, the Non-line-of-sight (NLOS) path loss channel model in [34] is applied and given by

$$\begin{aligned} G_D(x)[\mathrm{dB}] = &- \left[44.9 - 6.55 \log_{10}(h_{BS})\right] \log_{10}(x) \\ &- 34.46 - 5.83 \log_{10}(h_{BS}), \end{aligned} \tag{5}$$

where $h_{BS} = 25m$ is the height of the base station.

C. Maximum D2D distance

Given that each capillary UE automatically connects to the nearest D2D agent, all the UEs will be clustered in Voronoi cells. We denote the random variable R_1 as the distance from a capillary UE to its nearest D2D agent and R_2 as the distance from a D2D agent to the furthest capillary UE connecting to it. We first obtain the CDF of R_1 without macro cell boundary, i.e., infinite UEs following a PPP in an infinite plane, as follows,

$$\begin{aligned} F_{R_1}(r) = 1 - \Pr[R_1 > r] &= 1 - \left. \frac{(r^2 \pi \lambda_D)^x e^{-r^2 \pi \lambda_D}}{x!} \right|_{x=0} \\ &= 1 - e^{-r^2 \pi \lambda_D}, \end{aligned} \tag{6}$$

where λ_D is the density of the D2D agents.

Theorem 1. *Given an infinite number of D2D agents and capillary UEs following the PPP with density λ_D and $\lambda - \lambda_D$, respectively, the CDF of the distance from a randomly chosen D2D agent to the furthest capillary UE connecting to it, R_2, is bounded by*

$$\begin{aligned} F_{R_2}(r) &> \sum_{n=0}^{\infty} \Pr[M = n] F_{R_1}(r)^n \\ &= \sum_{n=0}^{\infty} \frac{3.5^{3.5} \Gamma(n + 3.5) (\lambda - \lambda_D/\lambda_D)^n (1 - e^{-r^2 \pi \lambda_D})^n}{n! \Gamma(3.5) (\lambda - \lambda_D/\lambda_D + 3.5)^{n+3.5}} \\ &= \hat{F}_{R_2}(r), \end{aligned} \tag{7}$$

where λ is the density of the UEs, including the D2D agents and capillary UEs, and M is the number of the capillary UE in a Voronoi cell.

Proof: See Appendix A in [35]. ■

When the size of each Voronoi cell is relatively small comparing with that of the macro cell, the proportion of the Voronoi cells cut by the macro cell boundary is small, so that (7) can well approximate the realistic situation that UEs are within a finite-size cell. We fix the radius of the macro cell to 500m and decrease λ from 10^{-1} to 10^{-3}. From Figs. 4 (a), (b), and (c), the gap between Monte Carlo results and the lower-bound in the infinite plane increase because a larger proportion of the Voronoi cells are affected by the macro cell boundary.

Because the LTE uplink Open-loop Fraction Power Control (OFPC) scheme is used to determine the D2D transmitting power, the longer the D2D distance, the higher the transmitting power and interference. Thus, we apply the lower-bound $\hat{F}_{R_2}(r)$ in Theorem 1 for the following analysis, which overestimates the maximum D2D distance and can be used to calculate the upper-bound of the D2D interference. By applying the upper-bound of the D2D interference, the analysis

This article has been accepted for publication in a future issue of this journal, but has not been fully edited. Content may change prior to final publication. Citation information: DOI 10.1109/TWC.2018.2817481, IEEE Transactions on Wireless Communications

in this paper reveals the minimum performance gain that can be achieved by the proposed schemes. The corresponding Probability Density Function (PDF) is obtained as follows,

$$\begin{aligned}\hat{f}_{R_2}(r) &= \frac{\mathrm{d}\hat{F}_{R_2}(r)}{\mathrm{d}r} \\ &= \sum_{n=0}^{\infty} \Pr[M=n] n F_{R_1}(r)^{n-1} f_{R_1},\ r>0, \end{aligned} \quad (8)$$

where the Probability Mass Function (PMF) of M is given by (35) in [35]. $\hat{f}_{R_2}(0)$ is an impulse function and can be obtained as follows,

$$\begin{aligned}\hat{f}_{R_2}(0) =& \Pr[M=n] \lim_{r\to 0} \frac{\frac{\mathrm{d}}{\mathrm{d}r}\left[n2\pi\lambda_D r e^{-r^2\pi\lambda_D}\right]}{\frac{\mathrm{d}}{\mathrm{d}r}\left[1-e^{-r^2\pi\lambda_D}\right]}\Bigg|_{n=0} \\ =& \Pr[M=0]. \end{aligned} \quad (9)$$

D. D2D transmitting power

In [34], the OFPC scheme is given by

$$P_{D2D} = \min\{P_{\max}, P_0 + 10\log_{10} T + \alpha PL_{D2D}\}, \quad (10)$$

where $P_{\max}$ denotes the maximum UE transmitting power. P_0 and T are configured by the eNB and are given in Table I. $PL_{D2D}(r)$ is the path loss between the D2D pair. α is selected from $[0,1]$ to determine the compensation weight of the path loss [36].

Considering the fact that most of the MTC devices are placed in the indoor environment, we assume that all the D2D transmissions experience the NLOS channels and the PL_{D2D} can be obtained based on the distance between the D2D agent and the capillary UE, d_{d2d}, as follows [34],

$$PL_{D2D}(d_{d2d})(\mathrm{dB}) = 36.8\log_{10}(d_{d2d}) + 43.8. \quad (11)$$

For the MTC small-data traffic, we use the distance from a D2D agent to its furthest capillary UE, R_2, to determine the D2D transmitting power (mW) as follows,

$$P_{D2D} = 10^{0.1\min\{24, -78+\alpha(36.8\log_{10}(R_2)+43.8)\}}. \quad (12)$$

E. D2D Interference

In this paper, we apply a simple rule to model the resource allocation for the D2D transmissions. In order to make a fair comparison with the current mechanism, the resource consumed for the MTC packets exchanging in the D2D network should be smaller than that for the same packets transmitting in the cellular uplink. In other words, the D2D transmission will be underlaid with the cellular transmissions for the same traffic without occupying additional cellular resource.

First, we use the received SNR (without the D2D interference) in the eNB side to perform the macro cell scheduling and then determine the MCS for the scheduled UE/Voronoi cell based on the SNR and estimated D2D interference level. We assume that the D2D transmission cannot use the last OFDM symbol of each subframe where UEs will transmit Sounding Reference Signal (SRS) for the uplink channel estimation, so that the eNB can still obtain the precise SNR of each UE. In order to ensure that all the D2D transmissions will be underlaid with the cellular transmissions, the number of D2D transmissions that could coexist per subframe, $\Omega^{(nc)}(M, MCS_i)$, in the NC scheme is given by

$$\Omega^{(nc)}(M, MCS_i) = \frac{2M+1}{M+1} MCS_i, \quad (13)$$

where MCS_i is the MCS selected by the eNB for a specific Voronoi cell, which means i packets/linear combinations can be transmitted in one PRB in the cellular uplink. In the NC scheme, as shown in Fig. 1 (a), there are two phases for the D2D transmissions, the D2D data collection and the D2D broadcasting. If there are totally M capillary UEs plus one D2D agent in the scheduled Voronoi cell, $2M+1$ D2D transmissions should be performed. We assume that each D2D transmission can only transmit one packet at one subframe. For example, when MCS_1 is selected, it needs $M+1$ cellular transmissions so that there should be $\frac{2M+1}{M+1}$ concurrent D2D transmissions on average in each subframe.

In practice, when MCS_0 is selected (SNR is too low and no transmission can succeed) for the cellular uplink, we can still allocate several concurrent D2D transmissions because they will not degrade the cellular transmission. Thus, (13) is the upper bound of the number of the concurrent D2D transmissions. Similarly, for the RUR scheme, the upper bound of the number of the concurrent D2D transmissions can be given as follows,

$$\Omega^{(rur)}(M, MCS_i) = \frac{M}{M+1} MCS_i. \quad (14)$$

We only obtain the distribution of the maximum D2D distance for the Voronoi cells that have at least one capillary UE, so that we are using the conditional PDF of R_2, which is

$$\hat{f}_{R_2}(r \mid r>0) = \frac{\hat{f}_{R_2}(r)}{1-\Pr[M=0]}, \quad r>0. \quad (15)$$

We assume that all the UEs in a Voronoi cell have the same distance to the eNB. For a scheduled Voronoi cell with M capillary UEs and given that MCS_i is selected, the estimated D2D interference can be approximated as,

$$\begin{aligned} I_{D2D}(M, MCS_i) \approx \Omega^{(\cdot)}(M, MCS_i) \int_{D_0}^{D_R} G_D(x) f_d(x) \mathrm{d}x \\ \times \int_{0^+}^{\infty} P_{D2D}(r) \frac{\hat{f}_{R_2}(r)}{1-\Pr[M=0]} \mathrm{d}r, \end{aligned} \quad (16)$$

where $(\cdot)$ can be either (nc) or (rur). $f_d(x)$ is the PDF of the distance from a D2D agent to the eNB, $f_d(x) = 2x/(D_R^2 - D_0^2), x \in [D_R, D_0]$. D_R is the radius of the macro cell and D_0 is the guard distance between the D2D transmission and the eNB.

V. Performance Evaluation For The MTC Small-Data Traffic

In the MTC small-data traffic scenario, when a UE's buffer is empty, it will be removed from the scheduling list. Thus, the

This article has been accepted for publication in a future issue of this journal, but has not been fully edited. Content may change prior to final publication. Citation information: DOI 10.1109/TWC.2018.2817481, IEEE Transactions on Wireless Communications

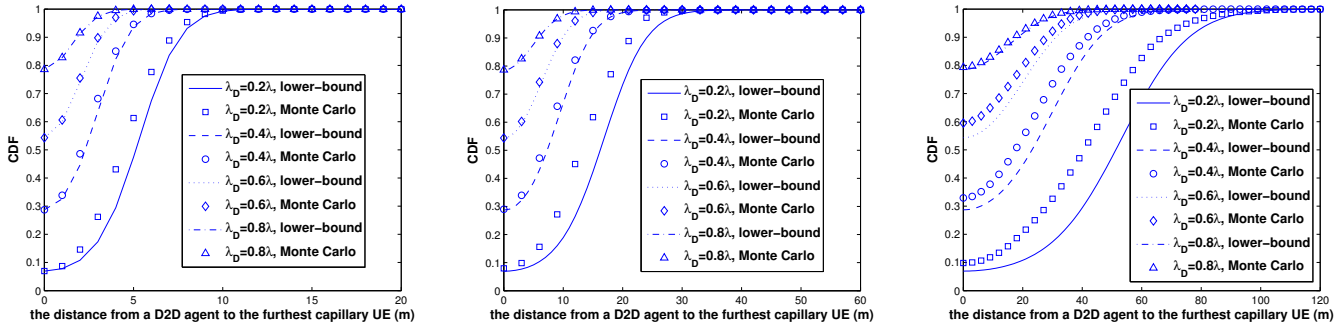

(a) $\lambda = 10^{-1}$ (b) $\lambda = 10^{-2}$ (c) $\lambda = 10^{-3}$

Fig. 4. Monte Carlo verification on the lower-bound of the CDF.

number and density of UEs are changing slot-to-slot, which brings difficulties to theoretical analysis and motivates the following Monte Carlo simulations.

A. Simulation Settings

TABLE I. PARAMETER SETTINGS

Parameters	Values	Description
λ	10^{-3}	The density of the UEs
λ_D	$a\lambda, a < 1$	The density of the D2D agents
D_0	300(m)	The minimum distance to the BS
D_R	500(m)	The maximum distance to the BS
A	$(D_R^2 - D_0^2)\pi/6$	The size of the simulation area
P_c	24(dBm)	The cellular transmitting power
B	1.8×10^5(Hz)	The bandwidth (1PRB)
N_0	$10^{-17.4}B$(mW)	Noise power
σ	0, 1, 2(dB)	Shadowing standard deviation
h_{BS}	25(m) [34]	The height of the BS
$P_{\max}$	24(dBm) [34]	Parameter in (10)
P_0	−78(dBm) [34]	Parameter in (10)
T	1 [34]	Parameter in (10)
α	0.7, 0.8, 0.9 [36]	Parameter in (10)

TABLE II. MCS TABLE

Order	MCS	SINR range (linear scale)
0	transmission failed	$(0, 0.6]$
1	QPSK, Rate 1/3	$(0.6, 2.135]$
2	QPSK, Rate 2/3	$(2.135, 4.565]$
3	16QAM, Rate 1/2	$(4.565, 8.584]$
4	16QAM, Rate 2/3	$(8.584, 13.583]$
5	16QAM, Rate 4/5	$(13.583, 19.498]$
6	64QAM, Rate 2/3	$(19.498, \infty)$

In the following simulation, we let all the UEs follow a PPP in a certain area A with the density λ, and randomly select D2D agents according to the probability a. Thus, all the D2D agents follow a PPP with the density λ_D, $\lambda_D = a\lambda$. The D2D transmitting power is determined based on the maximum D2D distance within the Voronoi cell, R_2. The D2D interference is generated according to the approximation in (16). The received SNR from each UE is generated as a random number based on the Rayleigh fast fading and the log-normal shadowing in each subframe. After the macro scheduling, the scheduled UE's signal-to-interference-plus-noise ratio (SINR) is calculated based on its SNR and the D2D interference. The MCS in this subframe is then determined according to the SINR. Each UE has a certain number of packets to be sent. The simulation ends once all the UEs' buffer become empty. We use the number of required cellular transmissions as the metric to evaluate the system because it represents the cellular resource consumption given the fixed bandwidth. The fewer the number of transmissions, the higher the transmission efficiency and the less the UE's power consumption. We define the gain as the ratio of the number of cellular transmissions that can be saved by the proposed scheme to the number of transmissions needed in the legacy LTE (i.e., without D2D), as shown in (17), and use it as the performance index in the following simulation.

$$\text{Gain} = 1 - \frac{\#\text{ of transmissions in the proposed scheme}}{\#\text{ of transmissions in LTE}}. \tag{17}$$

In the simulation, we adopt the same parameter settings, including topology, channel model, and transmitting power as summarized in Table I, for the proposed schemes and the legacy LTE. The Adaptive Modulation and Coding scheme (AMC) is adopted. The MCSs that can be selected in the simulation are shown in Table II [37]. The order of each MCS means the number of packets/linear combinations that can be transmitted by this MCS in one PRB. Based on the resource amount of one PRB and the resource occupied by the SRS and the Demodulation Reference Signal (DMRS) in the LTE uplink, the data amount of one MTC packet should be less than 88 bits. When the data amount of one UE is larger than 88 bits, it will be divided into several packets. Specifically, for the legacy LTE, the maximum applied MCS order cannot exceed the number of the packets per UE.

B. Simulation Results

As shown in Figs. 5, we set $\alpha = 0.8$, which is the compensation weight in (10). Fig. 5 (a) is the homogeneous case with no shadowing. Figs. 5 (b) and (c) are the heterogeneous cases with

This article has been accepted for publication in a future issue of this journal, but has not been fully edited. Content may change prior to final publication. Citation information: DOI 10.1109/TWC.2018.2817481, IEEE Transactions on Wireless Communications

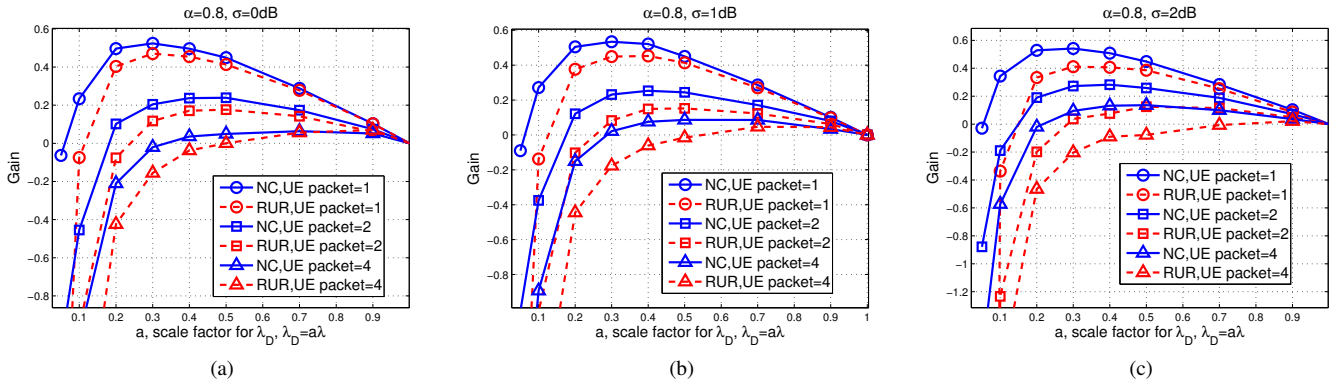

(a) (b) (c)

Fig. 5. Performances of different shadowing setting.

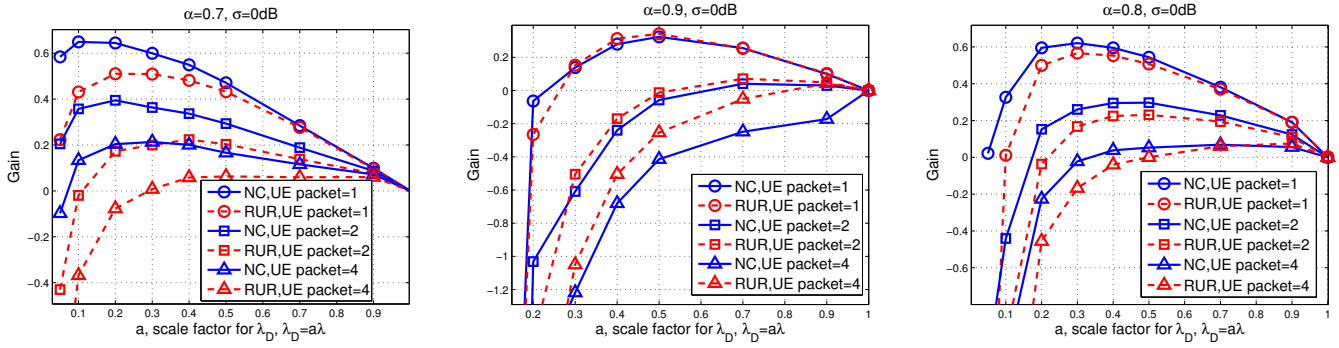

(a) (b) (c)

Fig. 6. Performances of different channel settings (Homogeneous).

the standard deviation of the shadowing equal to 1dB and 2dB, respectively. In these cases, when each UE has only one packet to send, more than 50% and 40% of cellular transmissions can be saved by the NC scheme and RUR scheme, respectively. The performance gain decreases with the growth of the data volume per UE.

Besides that, the NC scheme can achieve a higher performance gain when the standard deviation of the shadowing is larger. It is because the best channel in a Voronoi cell is always selected and thus a higher multi-user diversity gain can be obtained. For example, when the per-UE packet number is 1, the performance gain of the best point in the figure ($\lambda_D = 0.4$) is 46.87% for the homogeneous case. When the standard deviations of the shadowing are $\sigma = 1$dB and 2dB, the results are 48.78% ($\lambda_D = 0.4$) and 52.86% ($\lambda_D = 0.3$), respectively.

On the contrary, with a higher shadowing the performance gain of the RUR scheme is decreased. The reason is that a higher shadowing means a higher probability of a randomly selected D2D agent having a bad channel condition. Because this D2D agent is responsible to deliver packets from others, it will greatly degrade the system performance.

We also show the different results according to different D2D channel settings in Figs. 6. We use different α values in Table I. By comparing these 3 figures, i.e., Fig. 6 (a), Fig. 5 (a), and Fig. 6 (b), we can observe that with the increasing of α the optimal λ_D becomes larger.

Given a certain transmission distance, a larger α means a larger D2D transmitting power, which will generate more interference. λ_D is negatively correlated with the D2D transmission distance. Therefore, when the D2D transmitting power is increased due to a larger α, the transmission distance has to decrease to reduce the D2D transmitting power according to the OFPC and control the interference level. Thus, the optimal point is moving toward a larger λ_D.

With the increase of α, the difference between the two schemes is getting smaller, and eventually the RUR scheme becomes better than the NC scheme (when $\alpha = 0.9$). It is because the NC scheme needs additional D2D broadcasting stage, which generates a higher D2D interference. It brings a negative effect to the NC scheme when the D2D transmitting power is relatively high comparing with the noise power and the cellular transmitting power. In this case, the D2D interference has offset all of the multi-user diversity gain achieved by the NC scheme.

For the path loss model, we used the same model in Table 1.2 of [32] which skipped the effect of carrier frequency, $23\log(f_c/5)$, a constant term equal to zero when $f_c = 5$ GHz.

This article has been accepted for publication in a future issue of this journal, but has not been fully edited. Content may change prior to final publication. Citation information: DOI 10.1109/TWC.2018.2817481, IEEE Transactions on Wireless Communications

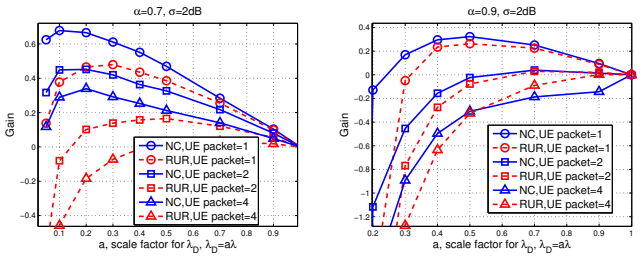

(a) (b)

Fig. 7. Performances of different D2D channel setting (Heterogeneous).

In Fig. 6 (c), f_c is chosen to be 2.6 GHz for comparison. We can observe that the trend in Fig. 6 (c) is similar to that in Fig. 5 (a) and the gains with 2.6 GHz carrier frequency increase slightly thanks to a smaller path loss and thus a higher small data aggregation gain. In practice, by applying the framework in this paper, no matter how the channel model varies, we can always identify the best method from NC, RUR, and legacy LTE, and approximately find the optimal density of the D2D agents.

Figs. 7 repeat the simulations in Figs. 6 (a) & (b) but with an on-average 2dB shadowing. The trends are similar, where the optimal λ_D is getting larger with the increasing of the D2D transmitting power. Also, the conclusion observed from Figs. 5 is confirmed again, i.e., the NC scheme can obtain a higher gain in the heterogeneous case.

In summary, the RUR scheme is preferable if the standard deviation of the shadowing is small and the D2D transmitting power is high, and vice versa. For both of the two schemes, the optimal density of the D2D agents can be approximately identified by the simulation results as well.

VI. Theoretical Analysis For The Full-Buffer Traffic

We applied Monte Carlo simulations for the MTC small-data traffic scenario because the topology and the scheduling list are changing which make it difficult to analyze. In the full-buffer traffic scenario, UEs always have data to transmit and they will not be removed from the scheduling list. Thus, the topology of the network and the scheduling list are stable, which facilitates us to provide theoretical analysis and gain deeper insights in this section. Different from using the times required for completing a transmission as the metric in the Monte Carlo simulations for the MTC small-data traffic, the received SINR at the eNB side is considered as the metric for the full-buffer traffic. The performance evaluation is then decoupled with detailed MCS table and target Block Error Ratio (BLER) setting.

In this section, we apply the same channel models used for the MTC small-data traffic, which are given by (3). In order to further reduce the feedback load, it is assumed that the UE with the best large-scale channel gain in a Voronoi cell will be always scheduled, because in this way the eNB does not need to frequently monitor the fast fading of each UE.

We fix the number of the capillary UEs in the ith Voronoi cell to M, so that the CDF and PDF of the SNR with the best large scale channel gain is given by

$$F_{\bar{\gamma}^{(*,i)}}(x \mid d_i, M) = F_{\bar{\gamma}_j}(x \mid d_i)^{M+1} = \Phi\left(\frac{10\log_{10} x/\bar{\gamma}(d_i)}{\sigma}\right)^{M+1}, \quad (18)$$

$$f_{\bar{\gamma}^{(*,i)}}(x \mid d_i, M) = \frac{\mathrm{d}F_{\bar{\gamma}^{(*,i)}}(x \mid d_i, M)}{\mathrm{d}x} = \frac{10(M+1)}{\sigma x \ln 10}\phi\left(\frac{10\log_{10} x/\bar{\gamma}(d_i)}{\sigma}\right)\Phi\left(\frac{10\log_{10} x/\bar{\gamma}(d_i)}{\sigma}\right)^{M}, \quad (19)$$

where $\phi(\cdot)$ is the PDF of the standard normal distribution. We apply the same scheduling scheme as that used for the MTC small-data traffic, i.e., the normalized SNR scheduling is applied in the macro cell and the Max C/I scheduling is used inside a Voronoi cell.

A. Network Coding

Theorem 2. *Given the full-buffer traffic and the NC scheme, the CDF of the received SNR at the eNB side from the ith Voronoi cell is given by*

$$F^{nc}_{\gamma^{(**,i)}}(x \mid d_i) = \sum_{l=1}^{\infty}\left[\sum_{m=0}^{\infty}\Pr[M=m]\int_0^{\infty}\left(1-e^{-\frac{x}{u}}\right)^l f_{\bar{\gamma}^{(*,i)}}(u \mid d_i, m)\mathrm{d}u\right] \times \frac{(\lambda_D A)^l e^{-\lambda_D A}}{l!\left(1-e^{-\lambda_D A}\right)}, \quad (20)$$

where the PMF of M, $\Pr[M=n]$, is given by (35) in [35], and A is the area of the macro cell.

Proof: We first assume that there are totally L equivalent UEs in the macro cell which also equals the number of Voronoi cells. The PDF of the SNR of each equivalent UE will be the same as that of the best UE in a Voronoi cell. Therefore, the conditional CDF of the received SNR at the eNB side from the ith Voronoi cell, $\gamma^{(**,i)}$, is given by

$$\begin{aligned} &F^{nc}_{\gamma^{(**,i)}}(x \mid d_i, \bar{\gamma}^{(*,i)}, M, L) \\ =&\Pr[\gamma^{(**,i)} < x \mid \text{the } i\text{th equivalent UE is selected}] \\ =&\frac{\Pr[\gamma^{(*,i)} < x, \frac{\gamma^{(*,i)}}{\bar{\gamma}^{(*,i)}(M)}\text{is max}]}{\Pr[\frac{\gamma^{(*,i)}}{\bar{\gamma}^{(*,i)}(M)}\text{is max}]} \\ =&\frac{\int_0^{\overline{\bar{\gamma}^{(*,i)}(M)}^{x}} f_{\frac{\gamma^{(*,i)}}{\bar{\gamma}^{(*,i)}}}(r \mid d_i)\prod_{\substack{j=1\\ j\neq i}}^{L} F_{\frac{\gamma^{(*,j)}}{\bar{\gamma}^{(*,j)}}}(r \mid d_i)\,\mathrm{d}r}{\int_0^{\infty} f_{\frac{\gamma^{(*,i)}}{\bar{\gamma}^{(*,i)}}}(r \mid d_i)\prod_{\substack{j=1\\ j\neq i}}^{L} F_{\frac{\gamma^{(*,j)}}{\bar{\gamma}^{(*,j)}}}(r \mid d_i)\,\mathrm{d}r}, \end{aligned} \quad (21)$$

where $\gamma^{(*,i)}$ and $\bar{\gamma}^{(*,i)}$ are the SNR and average SNR of the best UE in the ith Voronoi cell, respectively. $f_{\frac{\gamma^{(*,i)}}{\bar{\gamma}^{(*,i)}}}(\cdot)$ and $F_{\frac{\gamma^{(*,j)}}{\bar{\gamma}^{(*,j)}}}(\cdot)$ are the PDF and CDF of the normalized SNR of the best UE in the ith and jth Voronoi cell, respectively. $\bar{\gamma}^{(*,i)}(M)$ means the average SNR, a function of the number

This article has been accepted for publication in a future issue of this journal, but has not been fully edited. Content may change prior to final publication. Citation information: DOI 10.1109/TWC.2018.2817481, IEEE Transactions on Wireless Communications

of capillary UEs in the ith Voronoi cell. Thus, we first obtain the normalized SNR's PDF of the best UE in the ith Voronoi cell given M.

$$\begin{aligned} &f_{\frac{\gamma^{(*,i)}}{\bar{\gamma}^{(*,i)}}}(r \mid d_i, M) \\ =&f_{\gamma^{(*,i)}}(\bar{\gamma}^{(*,i)}(M)r \mid d_i)\left|\frac{\mathrm{d}}{\mathrm{d}r}\left(\bar{\gamma}^{(*,i)}(M)r\right)\right| = e^{-r}. \end{aligned} \quad (22)$$

The CDF can be obtained as follows,

$$F_{\frac{\gamma^{(*,i)}}{\bar{\gamma}^{(*,i)}}}(r \mid d_i, M) = \int_0^r f_{\frac{\gamma^{(*,i)}}{\bar{\gamma}^{(*,i)}}}(x \mid d_i, M)\mathrm{d}x = 1 - e^{-r}. \quad (23)$$

It is clear that (22) and (23) are not related to d_i or M, which means that the distribution of the best UE's normalized SNR is i.i.d. for different Voronoi cells, so that we can change the notations of $f_{\frac{\gamma^{(*,i)}}{\bar{\gamma}^{(*,i)}}}(r \mid d_i)$ and $F_{\frac{\gamma^{(*,j)}}{\bar{\gamma}^{(*,j)}}}(r \mid d_i)$ in (21) to $f_{\frac{\gamma^{(*)}}{\bar{\gamma}^{(*)}}}(r)$ and $F_{\frac{\gamma^{(*)}}{\bar{\gamma}^{(*)}}}(r)$, respectively. Therefore, (21) is rewritten as follows,

$$\begin{aligned} &F^{nc}_{\gamma^{(**,i)}}(x \mid d_i, \bar{\gamma}^{(*,i)}, M, L) \\ =&\frac{\int_0^{\frac{x}{\bar{\gamma}^{(*,i)}(M)}} f_{\frac{\gamma^{(*)}}{\bar{\gamma}^{(*)}}}(r)\prod_{\substack{j=1\\ j\neq i}}^{L} F_{\frac{\gamma^{(*)}}{\bar{\gamma}^{(*)}}}(r)\mathrm{d}r}{\int_0^{\infty} f_{\frac{\gamma^{(*)}}{\bar{\gamma}^{(*)}}}(r)\prod_{\substack{j=1\\ j\neq i}}^{L} F_{\frac{\gamma^{(*)}}{\bar{\gamma}^{(*)}}}(r)\mathrm{d}r} \\ =&\frac{\frac{1}{L}\left[F_{\frac{\gamma^{(*)}}{\bar{\gamma}^{(*)}}}(\frac{x}{\bar{\gamma}^{(*,i)}(M)})\right]^L}{\frac{1}{L}\left[F_{\frac{\gamma^{(*)}}{\bar{\gamma}^{(*)}}}(\frac{y}{\bar{\gamma}^{(*,i)}(M)})\right]^L\Big|_0^{\infty}} = \left[F_{\frac{\gamma^{(*)}}{\bar{\gamma}^{(*)}}}(\frac{x}{\bar{\gamma}^{(*,i)}(M)})\right]^L. \end{aligned} \quad (24)$$

The conditional distribution of the average SNR of the best UE in this Voronoi cell, $\bar{\gamma}^{(*,i)}$, can be found in (19), we remove the conditions of $\bar{\gamma}^{(*,i)}$ and M successively,

$$\begin{aligned} &F^{nc}_{\gamma^{(**,i)}}(x \mid d_i, M, L) \\ =&\int_0^{\infty}\left[F_{\frac{\gamma^{(*)}}{\bar{\gamma}^{(*)}}}(\frac{x}{u})\right]^L f_{\bar{\gamma}^{(*,i)}}(u \mid d_i, m)\mathrm{d}u. \end{aligned} \quad (25)$$

$$F^{nc}_{\gamma^{(**,i)}}(x \mid d_i, L) = \sum_{m=0}^{\infty}\Pr[M=m]F^{nc}_{\gamma^{(**,i)}}(x \mid d_i, M, L). \quad (26)$$

Assuming that there is at least one D2D agent existing, the condition of L in (26) can be further removed as shown below. According to the PPP model, $\Pr[L=l] = \frac{(\lambda_D A)^l e^{-\lambda_D A}}{l!}$. By substituting (26) into (27), Theorem 2 can be obtained.

$$F^{nc}_{\gamma^{(**,i)}}(x \mid d_i) = \sum_{l=1}^{\infty} F^{nc}_{\gamma^{(**,i)}}(x \mid d_i, l)\frac{\Pr[L=l]}{1-\Pr[L=0]}. \quad (27)$$

■

B. Random UE Relay

Theorem 3. *Given the full-buffer traffic and the RUR scheme, the CDF of the received SNR at the eNB side from the ith Voronoi cell is given by*

$$\begin{aligned} &F^{rur}_{\gamma^{(**,i)}}(x \mid d_i) \\ =&\sum_{n=1}^{\infty}\frac{(\lambda_D A)^n e^{-\lambda_D A}}{n!\,(1-e^{-\lambda_D A})}\int_0^{\infty}\left(1-e^{-\frac{x}{u}}\right)^n f_{\bar{\gamma}_i}(u \mid d_i)\mathrm{d}u. \end{aligned} \quad (28)$$

where the PMF of M, $\Pr[M=n]$, is given by (35) in [35], and A is the area of the macro cell.

Proof: In the RUR scheme, the eNB cannot select the best UE in a Voronoi cell, so that the CDF of the received SNR at the eNB side of the randomly selected UE in the ith Voronoi cell can be given by (3). The CDF of the normalized SNR of the randomly selected UE in a Voronoi cell can be easily obtained as follows, which is the same as that of the NC scheme and is also i.i.d.. The condition of the distance from the ith Voronoi cell to the eNB, d_i, can be removed.

$$F_{\frac{\gamma_i}{\bar{\gamma}_i}}(x \mid d_i) = 1 - e^{-x} = F_{\frac{\gamma}{\bar{\gamma}}}(x). \quad (29)$$

After the macro cell scheduling, the CDF of the received SNR in the eNB side from the ith Voronoi cell is given by

$$\begin{aligned} F^{rur}_{\gamma^{(**,i)}}(x \mid d_i) =&\sum_{n=1}^{\infty}\frac{\Pr[L=n]}{1-\Pr[L=0]} \\ &\times\int_0^{\infty}\left[F_{\frac{\gamma}{\bar{\gamma}}}(\frac{x}{u})\right]^n f_{\bar{\gamma}_i}(u \mid d_i)\mathrm{d}u. \end{aligned} \quad (30)$$

In the RUR case, we use the PDF of one single UE's average SNR $f_{\bar{\gamma}_i}(\cdot)$ instead of that of the best UE. By substituting (29) into (30), Theorem 3 can be obtained. ■

C. Legacy System Without Cooperation

If there is no cooperation among UEs, only the macro scheduling will be performed and the eNB will always schedule the UE with the largest normalized SNR as shown in (1). The distribution of received SNR at the eNB side is similar to that of the RUR scheme. The difference is that the user number in the macro scheduling list does not equal the number of the D2D agents in the RUR scheme but equals the overall UE number in the legacy system.

Therefore, the CDF of the received SNR in the eNB side from the ith UE can be given by

$$\begin{aligned} F^{l}_{\gamma^{(**,i)}}(x \mid d_i) =&\sum_{n=1}^{\infty}\frac{\Pr[U=n]}{1-\Pr[U=0]} \\ &\times\int_0^{\infty}\left[F_{\frac{\gamma}{\bar{\gamma}}}(\frac{x}{u})\right]^n f_{\bar{\gamma}_i}(u \mid d_i)\mathrm{d}u, \end{aligned} \quad (31)$$

where U is the overall UE number and the PMF is given by $\Pr[U=n] = \frac{(\lambda A)^n e^{-\lambda A}}{n!}$.

This article has been accepted for publication in a future issue of this journal, but has not been fully edited. Content may change prior to final publication. Citation information: DOI 10.1109/TWC.2018.2817481, IEEE Transactions on Wireless Communications

D. D2D Interference

The maximum D2D distance is applied to calculate the D2D transmitting power for the MTC small-data traffic because the power control may not be performed in time and precisely for bursty traffic. However, the transmission is continuous in the full-buffer scenario, and thus a more precise power control can be achieved. Therefore, we apply the OFPC scheme combined with the distance from a capillary UE to the nearest D2D agent, which is denoted as R_1 in Sec. IV-C, and whose CDF is given by (6), to calculate the D2D transmitting power for the full-buffer traffic. The PDF of R_1 is given by $f_{R_1}(r) = \frac{\mathrm{d}F_{R_1}(r)}{\mathrm{d}r} = 2\pi r\lambda_D e^{-r^2\pi\lambda_D}$.

Given the arbitrary shape of cooperative area in practice, we use the PDF of R_1 in an infinite plane to approximate the D2D interference from a single source by

$$I_s \approx \int_{D_0}^{D_R} G_D(x) f_d(x) \mathrm{d}x \int_0^{\infty} P_{D2D}(r) f_{R_1}(r) \mathrm{d}r, \quad (32)$$

where $G_D(x)$, $P_{D2D}(r)$ can be found in (5) and (10), respectively.

For D2D links, besides the NLOS channel model used in (11), the Line-Of-Sight (LOS) D2D channel is also considered in the performance evaluation of the full-buffer traffic, which is suitable for the devices in the outdoor scenarios and non-MTC scenarios. The path loss model [34] in dB scale is given by $PL_{D2D}(R_1) = 18.7\log_{10}(R_1) + 46.8$. The different models lead to different D2D transmitting power and interference level, which will make a big difference on the performance gains in the following numerical evaluations. Other than applying a specific MCS table for the MTC small-data traffic, we use another model to facilitate the evaluations of the theoretical results for the full-buffer traffic.

The number of concurrent D2D transmissions are highly related to the data rate in the macro cell. In a Voronoi cell, the D2D transmissions for certain packets should be finished before their cellular transmissions, so that the cooperation schemes can work. The D2D transmissions in one Voronoi cell can be underlaid with the cellular transmissions of other Voronoi cells. When the traffic arrival is continuous, the procedure above can be wrapped around. Overall, the D2D transmissions cannot occupy more time-frequency resource than that used by the cellular transmissions for the same amount of data. Therefore, the higher data rate in cellular, the less resource can be utilized for the D2D transmission.

In the RUR scheme, the D2D agent will collect the packets from other capillary UEs. If the data amount of each UE is s, the total data amount to be transmitted via the D2D in this Voronoi cell is sM. The data amount for the cellular uplink transmission is $s(M+1)$ because the D2D agent also has its own traffic. The ratio of the traffic amount in the D2D and the cellular is $M/(M+1)$, which is approximated to be 1 for simplicity. In other words, if the data rates in the D2D and the cellular are the same, $\Omega^{rur} = 1$. If the data rate in the cellular is c times of that in the D2D, $\Omega^{rur} = c$. In the NC scheme, the D2D agent has to broadcast all of the packets back to each capillary UE, so that the ratio of the traffic amount in the D2D and the cellular is $(2M+1)/(M+1)$, which can be approximated as twice of that of the RUR scheme.

The number of concurrent D2D transmissions is also related to the D2D resource allocation scheme, i.e., whether the D2D transmissions are exactly underlaid with the cellular uplink transmissions. If some of the D2D transmissions are offloaded to D2D dedicated resource or an unlicensed band, the number of concurrent D2D transmissions can be reduced.

Since the D2D resource allocation scheme is not the main focus of this paper, we use the extreme cases to evaluate the range of the performance gain of the proposed solutions. For example, we assume that the MCS of QPSK and $1/3$ coding rate is adopted for the D2D transmission, which has the lowest modulation order and a relatively low coding rate in the LTE uplink. In the cellular, if the average MCS can be as low as that of the D2D transmission or part of the D2D transmissions can be offloaded to another resource, the D2D concurrent transmission number will be much smaller, even zero.

We assume $\Omega^{rur} = 1$, $\Omega^{nc} = 2$ for the out-of-band D2D allocation case. If we select $\Omega^{rur} = 5$, $\Omega^{nc} = 10$, it means that all of the D2D transmissions can be underlaid with the cellular uplink and the average MCS of the cellular should be at least 64QAM and $1/2$ coding rate, which is the maximum modulation order in the LTE uplink and we believe that is large enough for the average MCS in the cellular for most of the cases. Therefore, the total D2D interference level can be approximated as $I_{D2D}^{(\cdot)} = \Omega^{(\cdot)} I_s$, where $(\cdot)$ can be either (nc) or (rur). We adjust $\Omega^{(\cdot)}$ to evaluate the performance gains in the following evaluation part.

E. SINR

Given the CDF of received SNR of each scheme shown in Sec.VI-A, Sec.VI-B and Sec.VI-C, and the approximation of the D2D interference, we can obtain the CDF of received SINR for the NC scheme as follows,

$$F_{SINR}^{nc}(x \mid d_i) = F_{\gamma^{(**,i)}}^{nc}\left(\frac{N_0 + I_{D2D}^{nc}}{N_0} x \mid d_i\right). \quad (33)$$

Because there is no D2D interference introduced in the legacy system, so that we can use the CDF of the SNR in (31) directly. The CDF of received SINR for the RUR scheme can be obtained by the same equation but replacing $F_{\gamma^{(**,i)}}^{nc}(\cdot)$ and I_{D2D}^{nc} by $F_{\gamma^{(**,i)}}^{rur}(\cdot)$ and I_{D2D}^{rur}, respectively.

VII. Performance Evaluation For The Full-Buffer Traffic

A. Parameter Settings

We use the received SINR at the eNB side from one Voronoi cell as the metric to evaluate the performance. In practice, given a fixed MCS table and a target BLER, a higher SINR results in a higher MCS for the uplink transmission in the tagged Voronoi cell. Thus a higher overall throughput of the macro cell can be obtained because of the equal scheduling opportunity for each Voronoi cell given the normalized SNR scheduling.

This article has been accepted for publication in a future issue of this journal, but has not been fully edited. Content may change prior to final publication. Citation information: DOI 10.1109/TWC.2018.2817481, IEEE Transactions on Wireless Communications

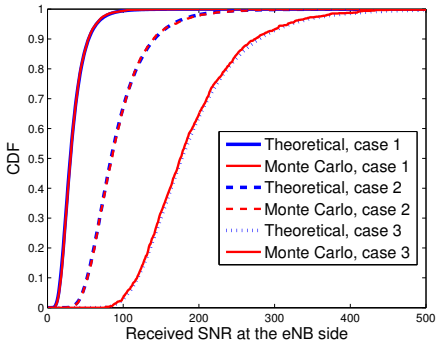

Fig. 8. Monte Carlo verification for Theorem 2.

Besides the SINR gain, the control overhead can be also reduced by the proposed cooperative transmission schemes. The data amount can be transmitted by each scheduling grant is increased because of the higher transmission efficiency. Thus given the same data amount, the number of needed scheduling messages is reduced. Another kind of control overhead is the feedback load, which can also be reduced due to the facts that only the large scale channel gains and the D2D agents' channels are monitored in the NC scheme and the RUR scheme, respectively.

Different from the scenario of MTC small-data traffic, there is no small-data aggregation gain for the full-buffer traffic. The RUR scheme cannot achieve a positive SINR gain but can reduce the queue length. The NC scheme can achieve a positive SINR gain thanks to the multi-user diversity gain, especially in the heterogeneous case when σ is large. We set $\sigma = 4$dB [34] for the full-buffer traffic in this section. Other parameters used in the numerical evaluation are the same with those summarized in Table I.

B. Monte Carlo Simulation

We have conducted Monte Carlo simulations to verify the key step of Theorem 2, i.e., eq. (25). The rest of proof procedures are just taking the expectation with respect to M and L. Three different cases are verified where $M = 5, 10, 20$ and $L = 20, 40, 100$, respectively. Because d_i only affects $\bar{\gamma}(d_i)$, we assume $\bar{\gamma}(d_i) = 5, 10, 15$ in the three cases. Other parameters are the same with those in Table I. As shown in Fig. 8, the theoretical results match well with the results of Monte Carlo simulations. Because Theorem 3 and the result of legacy LTE adopt the same method and reuse the key part of Theorem 2, they can be verified by the same Monte Carlo simulations as well.

C. Numerical Results

The LOS D2D channel model is first applied. We fix the distance from one Voronoi cell to the eNB to 500m and examine the CDF of the received SINR at the eNB side from this Voronoi cell. The scenarios with the highest D2D interference level are shown in Fig. 9 (b), where $\alpha = 0.9$ and

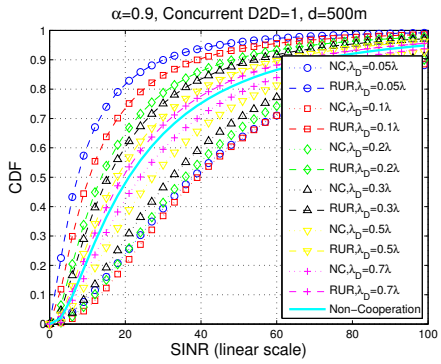

(a)

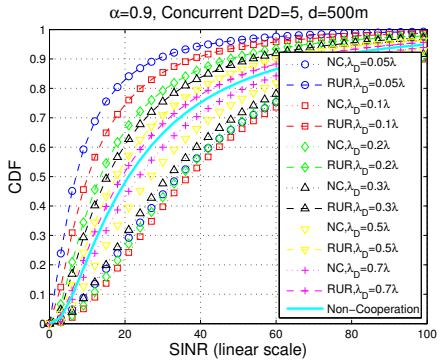

(b)

Fig. 9. Evaluation results of the LOS D2D channel, $d_i = 500$m.

is the largest option in Table I. According to the analysis in Sec. VI-D, $\Omega^{rur} = 5$ and $\Omega^{nc} = 2\Omega^{rur}$. Even in this less favourable case the NC scheme can still achieve a significant gain. For instance, the 50 percentile and 20 percentile of SINR is increased by 71% and 100%, respectively, comparing with the Non-Cooperation system. It means that the NC scheme is always a promising choice in the case of LOS D2D channel.

The NLOS D2D channel model is then applied. We choose the same settings for Ω^{nc} and Ω^{rur} but use different values of α. It can be observed from Figs. 10 that the SINR performances of the RUR scheme are worse than the legacy system (Non-Cooperation). It is because the number of users to be scheduled is decreased thus a part of the multi-user diversity gain is lost. Also, an additional D2D interference is introduced by the cooperative transmissions. With the increasing of λ_D, more D2D agents can be scheduled and less D2D interference will be introduced due to shorter distances between capillary UEs and D2D agents, the CDF of the RUR scheme is thus getting closer to that of the legacy system.

On the contrary, the NC scheme can achieve a positive performance gain in the most cases, especially when the D2D interference can be maintained in a relatively low level. As shown in Fig. 10 (a), a huge gain can be achieved. But with the rise of the D2D interference level (α and/or concurrent D2D number), the performance gain becomes smaller, as shown in Figs. 10 (b), (c) and (d). Eventually, there is no positive gain in Figs. 10 (e) and (f).

This article has been accepted for publication in a future issue of this journal, but has not been fully edited. Content may change prior to final publication. Citation information: DOI 10.1109/TWC.2018.2817481, IEEE Transactions on Wireless Communications

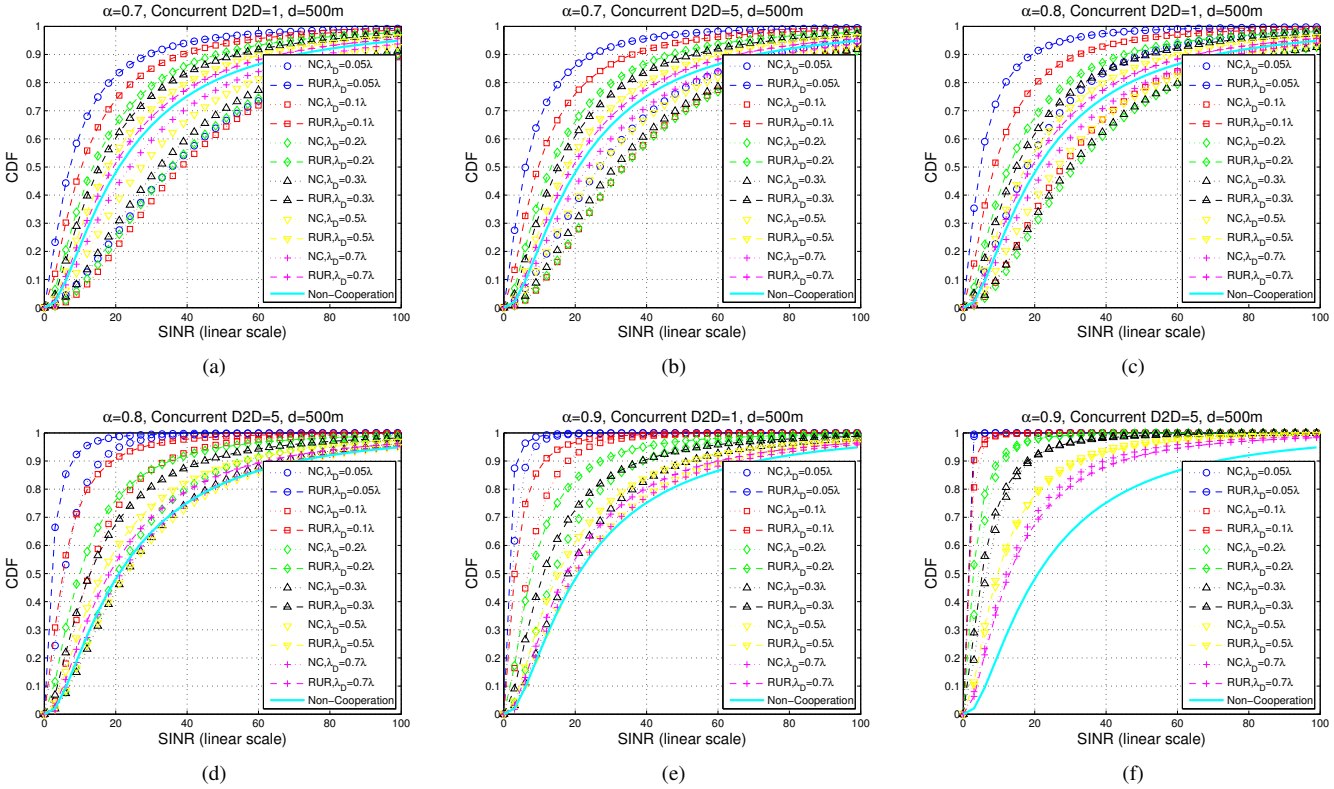

Fig. 10. Evaluation results of the NLOS D2D channel, $d_i = 500$m.

The benefit of the NC scheme comes from the best channel selection inside a Voronoi cell, which brings an additional multi-user diversity gain at the cost of the D2D interference. When the D2D transmitting power is low, the multi-user diversity gain will dominate and thus a SINR gain can be achieved. However, when the D2D interference is large enough, all of the multi-user diversity gain will be devoured by the interference.

As shown in Fig. 10 (a), the NC scheme can achieve the best performance when $\lambda_D = 0.1\lambda$. The difference between the curves of $\lambda_D = 0.1\lambda$ and $\lambda_D = 0.2\lambda$ becomes smaller when $\Omega^{(\cdot)}$ is increased in Fig. 10 (b). When $\alpha = 0.8$, the D2D interference level is further increased and 0.2λ is the best choice for λ_D as shown in Fig. 10. In the following figures, with the further increasing of the D2D interference level, the optimal λ_D is moving toward a larger value. It is because λ_D is negatively correlated with the distance between the capillary UEs and their D2D agents. Reducing the size of the Voronoi cells can compensate the increasing of the D2D interference.

The NC scheme cannot always achieve a better performance than the RUR scheme. For example, as shown in Fig. 10 (f), when $\lambda_D = 0.7\lambda$ the RUR scheme is better than the NC scheme. It is because that the D2D interference introduced by the NC scheme is twice of that of the RUR scheme. When the interference level is high, and there is not much multi-user diversity gain to be utilized by the NC scheme due to the limited capillary UE number in each Voronoi cell, the doubled D2D interference will make the difference.

Although the performances of the cooperative transmission schemes are worse than the legacy system in the high D2D interference level cases (Figs. 10 (e) and (f)), these evaluations are still valuable due to other benefits brought by the cooperative schemes, such as the scheduling list reduction. Our analysis provides a clear relationship between the performance degradation and the scheduling list reduction, which is a good reference for the eNB to make the trade-off. For example, if the eNB decides to reduce the scheduling queue length by 30% in the scenario of Fig. 10 (f), it is shown how much performance gain needs to be sacrificed, and it is clear that the RUR scheme is a better choice in this case.

As shown in Figs. 11, we repeat the numerical evaluations for the scenarios of $d_i = 300$m. It can be observed that the performance gain and the best λ_D are the same with the results in Figs. 10, but the absolute values of the SINR are significantly increased. It is because the D2D interference comes from the whole cell which is not related to the position of the tagged Voronoi cell. Therefore, only the received power from the tagged Voronoi cell is increased due to a shorter transmission distance and thus the SINR is also increased.

In summary, for the full-buffer traffic scenario, the NC scheme can always achieve a positive gain in the cases with LOS D2D channels or in the most cases with NLOS D2D channels. The numerical results provide a good guideline for the eNB to control the density of the D2D agents. The RUR scheme is a better choice if the eNB determines to reduce

This article has been accepted for publication in a future issue of this journal, but has not been fully edited. Content may change prior to final publication. Citation information: DOI 10.1109/TWC.2018.2817481, IEEE Transactions on Wireless Communications

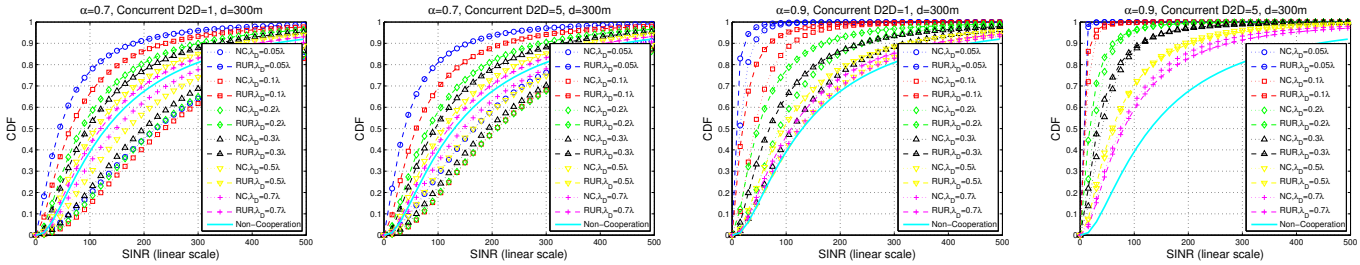

(a) (b) (c) (d)

Fig. 11. Evaluation results of the NLOS D2D channel, $d_i = 300$m.

the scheduling queue length and the feedback load at the cost of the performance degradation. The quantitative performance degradations are identified by the numerical results, and thus help the eNB to make the trade-off.

VIII. Conclusion

In this paper, a semi-centralized cooperative control method has been proposed for the cellular uplink transmission to address the new challenges brought by IoT, where the UE relays were randomly selected according to a certain density decided by the eNB. Two cooperative schemes based on the D2D have been proposed, which are the RUR scheme and the NC scheme. The proposed schemes have been analyzed given the D2D interference modeled by the stochastic geometry and two distinct traffic models, i.e., the MTC traffic with small-data feature and the full-buffer traffic. Intensive Monte Carlo simulations have been first conducted for the small-data traffic and then closed-form theoretical results have been derived for the full-buffer traffic. For both of the traffic models, the performance gains have been identified in various scenarios and the comparisons between two cooperative schemes have been made as well. Also, these results can provide an important guideline for the eNB to make the trade-off between the transmission efficiency and the scheduling queue length and to approximately determine the optimal density of the UE relays.

The current grouping method based on randomly selected D2D agents is efficient but not optimal. How to tune parameter a according to some UE-specific features, such as the UE's receiving power of the eNB's downlink pilot, to further optimize the grouping requires further investigation. In that way, the D2D agents may no longer follow a PPP, and some of the theoretical results in this paper need to be revisited. For the proposed schemes, the advantage of the control overhead reduction has not been quantified yet, which is worth studying in the future. Due to the heavy control/feedback overhead and high complexity of advanced multi-antenna techniques, we do not consider them in this paper. However, the trade-off between the high spectrum efficiency and the overhead may be an interesting further research issue. In this paper, the minimum performance gain based on extreme cases has be achieved, but the exact performance gain that can be obtained in reality is still an open issue. This part needs to consider the detailed scheduling algorithm design for the concurrent D2D transmissions, which plays an important role in the overall system performance and beckons for further investigation.

References

[1] Y. Li, M. Ghasemiahmadi, and L. Cai, "Uplink cooperative transmission for machine-type communication traffic in cellular system," in *Proc. of IEEE VTC-Fall*, 2016, pp. 1–5.

[2] ——, "Performance analysis of semi-centralized controlled uplink cooperative transmission," in *Proc. of IEEE GLOBECOM*, 2016, pp. 1–6.

[3] 3GPP, "Study on Enhancements to Machine-Type Communications (MTC) and other Mobile Data Applications; Release 12," 3rd Generation Partnership Project (3GPP), TR 37.869, 2013.

[4] ——, "Study on provision of low-cost Machine-Type Communications (MTC) User Equipments (UEs) based on LTE; Release 12," 3rd Generation Partnership Project (3GPP), TR 36.888, 2013.

[5] ——, "Service requirements for Machine-Type Communications (MTC); Stage 1; Release 13," 3rd Generation Partnership Project (3GPP), TS 22.368, 2014.

[6] ——, "Proximity-Based Services (ProSe); Stage 2; Release 12," 3rd Generation Partnership Project (3GPP), TS 23.303, 2014.

[7] L. Lei, Z. Zhong, C. Lin, and X. Shen, "Operator controlled device-to-device communications in LTE-advanced networks," *IEEE Wireless Commun.*, vol. 19, no. 3, 2012.

[8] A. T. Gamage, H. Liang, R. Zhang, and X. Shen, "Device-to-device communication underlaying converged heterogeneous networks," *IEEE Wireless Commun.*, vol. 21, no. 6, pp. 98–107, 2014.

[9] K. Vanganuru, S. Ferrante, and G. Sternberg, "System capacity and coverage of a cellular network with D2D mobile relays," in *Proc. of IEEE MILCOM*, 2012, pp. 1–6.

[10] S. Wen, X. Zhu, Y. Lin, Z. Lin, X. Zhang, and D. Yang, "Achievable transmission capacity of relay-assisted device-to-device (D2D) communication underlay cellular networks," in *Proc. of IEEE VTC-Fall*, 2013, pp. 1–5.

[11] B. Raghothaman, G. Sternberg, S. Kaur, R. Pragada, T. Deng, and K. Vanganuru, "System architecture for a cellular network with cooperative mobile relay," in *Proc. of IEEE VTC-Fall*, 2011, pp. 1–5.

[12] K. Vanganuru, M. Puzio, G. Sternberg, K. Shah, and S. Kaur, "Uplink system capacity of a cellular network with cooperative mobile relay," in *Proc. of IEEE WTS*, 2011, pp. 1–7.

[13] M. Ni, L. Zheng, F. Tong, J. Pan, and L. Cai, "A geometrical-based throughput bound analysis for device-to-device communications in cellular networks," *IEEE J. Sel. Areas Commun.*, vol. 33, no. 1, pp. 100–110, 2015.

[14] F. Tong, Y. Wan, L. Zheng, J. Pan, and L. Cai, "A probabilistic distance-based modeling and analysis for cellular networks with underlaying device-to-device communications," *IEEE Trans. Wireless Commun.*, vol. 16, no. 1, pp. 451–463, 2017.

[15] L. Wang, T. Peng, Y. Yang, and W. Wang, "Interference constrained relay selection of D2D communication for relay purpose underlaying cellular networks," in *Proc. of IEEE WiCOM*, 2012, pp. 1–5.

[16] J. K. Sundararajan, D. Shah, M. Médard, S. Jakubczak, M. Mitzenmacher, and J. Barros, "Network coding meets TCP: Theory and implementation," *Proceedings of the IEEE*, vol. 99, no. 3, pp. 490–512, 2011.

[17] R. Ahlswede, N. Cai, S.-Y. Li, and R. W. Yeung, "Network information flow," *IEEE Trans. Inf. Theory*, vol. 46, no. 4, pp. 1204–1216, 2000.

[18] S.-Y. Li, R. W. Yeung, and N. Cai, "Linear network coding," *IEEE Trans. Inf. Theory*, vol. 49, no. 2, pp. 371–381, 2003.

[19] J. K. Sundararajan, D. Shah, and M. Médard, "ARQ for network coding," in *Proc. of IEEE ISIT*, 2008, pp. 1651–1655.

[20] T. Zhou, B. Xu, T. Xu, H. Hu, and L. Xiong, "User-specific link adaptation scheme for device-to-device network coding multicast," *IET Commun.*, vol. 9, no. 3, pp. 367–374, 2015.

[21] S. El Rouayheb, A. Sprintson, and P. Sadeghi, "On coding for cooperative data exchange," in *Proc. of IEEE ITW*, 2010, pp. 1–5.

[22] N. J. Hernandez Marcano, J. Heide, D. E. Lucani, and F. H. Fitzek, "On the throughput and energy benefits of network coded cooperation," in *Proc. of IEEE CloudNet*, 2014, pp. 138–142.

[23] A. Tassi, F. Chiti, R. Fantacci, and F. Schoen, "An energy efficient resource allocation scheme for RLNC-based heterogeneous multicast communications," *IEEE Commun. Letters*, vol. 18, no. 8, pp. 1399–1402, 2014.

[24] S. E. Tajbakhsh and P. Sadeghi, "Coded cooperative data exchange for multiple unicasts," in *Proc. of IEEE ITW*, 2012, pp. 587–591.

[25] Y. Li, K. Sun, and L. Cai, "Cooperative device-to-device communication with network coding for machine type communication devices," *IEEE Trans. Wireless Commun.*, vol. 17, no. 1, pp. 296–309, 2018.

[26] Y. Li, S. Zhu, and X. Guo, "System design for multiple users cooperative communication in LTE," in *Proc. of IEEE VTC-Fall*, 2013, pp. 1–5.

[27] A. Osseiran, K. Doppler, C. Ribeiro, M. Xiao, M. Skoglund, and J. Manssour, "Advances in device-to-device communications and network coding for IMT-advanced," *ICT Mobile Summit*, 2009.

[28] A. Abrardo, G. Fodor, and B. Tola, "Network coding schemes for device-to-device communications based relaying for cellular coverage extension," in *Proc. of IEEE SPAWC*, 2015, pp. 670–674.

[29] S. M. Yu and S.-L. Kim, "Downlink capacity and base station density in cellular networks," in *Proc. of IEEE WiOpt*, 2013, pp. 119–124.

[30] 3GPP, "Evolved Universal Terrestrial Radio Access (E-UTRA); Medium Access Control (MAC) protocol specification; Release 14," 3rd Generation Partnership Project (3GPP), TS 36.321, 2017.

[31] P. Viswanath, D. N. Tse, and R. Laroia, "Opportunistic beamforming using dumb antennas," *IEEE Trans. Inf. Theory*, vol. 48, no. 6, pp. 1277–1294, 2002.

[32] M. Torabi, W. Ajib, and D. Haccoun, "Performance analysis of rate-adaptive scheduling in MIMO systems with antenna selection," in *Proc. of IEEE PIMRC*, 2008, pp. 1–6.

[33] L. Yang and M.-S. Alouini, "Performance analysis of multiuser selection diversity," *IEEE Trans. Veh. Technol.*, vol. 55, no. 6, pp. 1848–1861, 2006.

[34] C. Xu, L. Song, and Z. Han, *Resource management for device-to-device underlay communication*. Springer, 2014.

[35] Y. Li. (2018) Cooperative device-to-device communication for uplink transmission in cellular system. [Online]. Available: http://web.uvic.ca/~liyue331/Report_UL_NC_D2D.pdf

[36] L. Ding, J. He, and Z. Liu, "A novel open loop power control method in LTE uplink," in *Proc. of IEEE WiCOM*, 2012, pp. 1–4.

[37] ITU. Link-level simulation results for IMT.EVAL. [Online]. Available: https://www.itu.int/oth/R0A06000025

Yue Li received his B.Sc. and M.Sc. degrees in electrical engineering from the Beijing Institute of Technology, Beijing, China, in 2006 and 2008, respectively. During 2008-2013, he worked for Huawei as a standard pre-research engineer in the Wireless Research Department. He has been closely involved in 3GPP standards evolvement and held numerous patents in WCMDA, LTE-A, and 5G systems. Currently he is a Ph.D. student in the Department of Electrical and Computer Engineering, University of Victoria, Victoria, Canada. His research interests include next-generation cellualr system, wireless network design and optimization, wireless system modeling and performance analysis.

Lin Cai Lin Cai (S'00-M'06-SM'10) received her M.A.Sc. and PhD degrees in electrical and computer engineering from the University of Waterloo, Waterloo, Canada, in 2002 and 2005, respectively. Since 2005, she has been with the Department of Electrical & Computer Engineering at the University of Victoria, and she is currently a Professor. Her research interests span several areas in communications and networking, with a focus on network protocol and architecture design supporting emerging multimedia traffic over wireless, mobile, ad hoc, and sensor networks.

She has served as a TPC symposium co-chair for IEEE Globecom'10 and Globecom'13. She served as an Associate Editor of the IEEE Transactions on Wireless Communications, IEEE Transactions on Vehicular Technology, EURASIP Journal on Wireless Communications and Networking, International Journal of Sensor Networks, and Journal of Communications and Networks (JCN), and as the Distinguished Lecturer of the IEEE VTS Society. She was a recipient of the NSERC Discovery Accelerator Supplement Grants in 2010 and 2015, respectively, and the Best Paper Awards of IEEE ICC 2008 and IEEE WCNC 2011. She has founded and chaired IEEE Victoria Section Vehicular Technology and Communications Joint Societies Chapter.